



Enhanced inulinase production by *Fusarium solani* JALPK from invasive weed using response surface methodology

Prajakta P. Kamble^a, Suresh S. Suryawanshi^b, Jyoti P. Jadhav^c, Yasmin C. Attar^{d,*}

^a Department of Microbiology, Shivaji University Kolhapur, 416004, India

^b Department of Biochemistry, Shivaji University Kolhapur, 416004, India

^c Department of Biotechnology, Shivaji University Kolhapur, 416004, India

^d Department of Microbiology, Rajaram College Kolhapur, 416004, India



ARTICLE INFO

Keywords:

Plackett–Burman design

Exoinulinase

Fructose

Box Behnken design

Tithonia rotundifolia

ABSTRACT

The present study is the first report of utilizing *Tithonia rotundifolia* weed as a substrate for inulinase production from *Fusarium solani* JALPK. It also deals with the statistical optimization of culture conditions to enhance the enzyme yield. Amongst the 11 variables screened by Plackett–Burman design, Inulin in combination with *Agave sisalana* extract, *Tithonia rotundifolia* extract and NaNO₃ had a significant influence on inulinase production and their concentrations were further optimized employing Box Behnken design. An enhancement of inulinase production from 970 EU/mL to 3261.011 EU/mL was gained after media optimization. Amongst the screened carbon sources *Tithonia rotundifolia* was found to be very effective in stimulating elevated inulinase synthesis. The *Tithonia rotundifolia* weed extract was treated with inulinase from *Fusarium solani* JALPK to form fructose which was estimated spectrophotometrically. This liberated fructose was also confirmed by osazone formation test and FTIR. HPTLC analysis of product revealed the exoinulinase nature of the enzyme produced by *Fusarium solani* JALPK since fructose was the only end product after hydrolysis of inulin rich weed in fermented broth. Thus the elevated extracellular inulinase yielding novel property of *Fusarium solani* JALPK (KY914560) contributes in considering it as a potential candidate with food, pharmaceutical and bioremediation applications.

1. Introduction

The Red sunflower: *Tithonia rotundifolia* (Mill.) S.F.Blake, an erect, large and robust seasonal bushy herb native to Mexico (Seiler, 2007) was deliberately introduced as ornamental plant in nearby regions of Kolhapur, India. However, in last few years *Tithonia rotundifolia* is drastically over spreading as a weed affecting the native varieties of plants (Howlett et al., 1973). The mechanical control of this weed is very ineffective due to its speedy adaptation and existence in rapidly changing environment (Muoghalu and Chuba, 2005). Thus, the increasing dominance of this inulin rich weed has forced us to develop novel strategies for controlling them by exploiting it as a potential renewable and abundant inulin rich substrate for inulinase production. Inulinase (exoinulinase: EC 3.2.1.26; β-D-fructofuranosidase or endoinulinase: EC 3.2.1.7; β-fructanfructanohydrolase) converts the inulin into fructose. Fructose thus formed is up to 2 times sweeter than table sugar, with great functional properties enhancing flavor, product stability and is extensively being used as an alternative to sucrose in beverages and numerous food products like breads, cereals, pastries,

candies, condiments, sodas and soft drinks, coffee drinks, cookies and cakes (Hanover and White, 1993). Many inulinase producing microorganisms like *Kluyveromyces*, *Aspergillus*, *Staphylococcus*, *Xanthomonas*, *Pseudomonas*, *Candida kefyr*, *Debaryomyces cantarelli*, *Penicillium*, and *Streptomyces sp* (Selvakumar and Pandey, 1999) were found to hydrolyze a variety of inulin rich plants including Jerusalem artichoke (*Helianthus tuberosus*), dahlia (*Dahlia*), elecampane (*Inula helenium*), chicory (*Cichorium*), dandelion (*Taraxacum*) and burdock (*Arctia*) (Kovaleva et al., 2009). But no literature is available till date regarding the use *Tithonia rotundifolia* as an inulin rich substrate for production of fungal inulinase. Hence, present study deals with the exploration of fungal inulinase for inulin rich weed management and its conversion into fructose of industrial value. Thereby reducing the development expenditure associated with fructose formation. This was achieved by employing sequential strategy of the experimental design for media optimization so as to obtain a significant increase in inulinase yields, making them commercially more attractive. Plackett–Burman Design was used to screen and identify the inulinase yield influencing media conditions in a single experiment. The key operational parameters

* Corresponding author.

E-mail address: ycamico@gmail.com (Y.C. Attar).

<https://doi.org/10.1016/j.mimet.2019.02.021>

Received 17 January 2019; Received in revised form 28 February 2019; Accepted 28 February 2019

Available online 02 March 2019

0167-7012/ © 2019 Elsevier B.V. All rights reserved.

screened for maximum fungal inulinase production were evaluated further by RSM using Box–Behnken Design which involves systematic and efficient variation of important components on the fermentation process.

The present investigation shows that Statistical media optimization of *Fusarium solani* JALPK inulinase used in bioconversion of inulin rich *Tithonia rotundifolia* into fructose has the potential to offer a number of benefits to food, drink and nutraceutical industries along with the weed management strategies.

2. Materials and methods

2.1. Collection of inulin rich substrates

Various inulin rich weeds were collected from different locations nearby Kolhapur District. *Agave sisalana* (16°28'32.8"N 74°10'31.0"E) stems were procured from mountain area in Walawa, Radhanagari, India. *Cosmos bipinnatus* Cav (16°40'43.6"N 74°15'05.9"E) and *Tithonia rotundifolia* (Mill.) S. F. Blake (16°40'55.7"N 74°15'07.4"E) was bought from Shivaji university campus, Kolhapur, India. All specimens were authentically identified and deposited at Herbarium, Department of Botany, Shivaji University, Kolhapur (Vouch. No.PPK03, PPK02, PPK01). Pure inulin (Chicory) and fructose were obtained from Himedia (Mumbai, India). All other chemicals used were of reagent grade.

2.2. Extraction of inulin from weed samples

The inulin was extracted from thoroughly washed, shredded, raw weed samples harvested at maturity, using a juice extractor, without adding extra water. The juices were clarified by centrifugation at 5000 rpm and concentrated supernatants were pre-treated at 70 °C in shaking water-bath for 10–15 min (Lingyun et al., 2007). After cooling, pH of these natural inulin extracts was adjusted to 6.5–7.0. The inulin content in this weed was estimated (Brkjjaca et al., 2014) and was near around 32%. The extract was stored at –20 °C until use.

2.3. Screening of inulinolytic fungal strain

A novel fungal strain, *Fusarium solani* JALPK with high extracellular inulinase producing ability, used in the present study was isolated from *Tithonia rotundifolia* rhizosphere soil. Preliminary screening of isolate was done by estimating inulinase activity and studying growth characters on inulin agar. While morphological characterization (colonial and microscopic properties) was performed on PDA (Hafizi et al., 2013). The strain was maintained at 4 °C on inulin agar (in g/L: KH₂PO₄ — 2.5; MgSO₄·7H₂O — 1.0; NaNO₃ — 20.0; Inulin — 20.0; agar — 20.0; pH — 6.0) after being incubated for 4 days at 30 °C and sub-cultured after every 3 weeks.

2.4. Molecular characterization and identification of potent inulinolytic fungal strain

Identification of the strain was done by performing 18S ribosomal RNA sequencing. The sequence alignment was performed using the Clustal W program (Thompson et al., 1994). The Translated nucleotide sequence was compared for similarity search with the fungal reference species present in genomic database banks by BLASTN tool (www.ncbi.nlm.nih.gov/BLAST) (Madden, 2013). The sequence was submitted to GenBank. Phylogenetic analysis of the aligned sequences was performed in Molecular Evolution Genetic Analysis (MEGA) software version 4.0 (Tamura et al., 2013). To deduce the evolutionary history, Bootstrap analysis was carried out using the neighbor-joining (NJ) algorithm (Saitou and Nei, 1987) and the evolutionary distances was calculated (Tamura et al., 2004).

2.5. Seed inoculum preparation

Vegetative inoculum was prepared by transferring one loop of mycelium growth from inulin agar medium in Erlenmeyer flasks (100 mL) containing 50 mL of the inulin broth and incubated at 30 °C with 120 rpm shaking for 96 h. The growth obtained was further transferred (2.5 mL spore suspension) in 250 mL Erlenmeyer flask, containing 150 mL production medium and cultivation was performed at 30 °C on a shaker, at 120 rpm for 96 h. The spores were harvested and counted by haemocytometer.

2.6. Inulinase production in submerged fermentation (SmF)

Submerged fermentation was carried out in 300 mL of fermentation medium supplemented with different carbon sources namely *Tithonia rotundifolia*, *Cosmos bipinnatus*, *Agave sisalana* and synthetic inulin. Medium was inoculated with 2% inoculum with 2×10^8 spores/mL and incubated at 30 °C with 120 rpm shaking for 96 h.

2.7. Inulinase assay

Synthetic inulin (2% in phosphate buffer pH 6.8) was used as the substrate for inulinase activity estimation. The mixture of enzyme solution (0.1 mL) and substrate (0.1 mL) was incubated at 30 °C for 20 min. After incubation, inulinase activity was determined by the method described by (Miller, 1959) with standard fructose as a reference compound. One unit of enzyme activity was defined as the amount of enzyme that catalyses the release of 1 μmol of fructose per minute per mL.

2.8. Evaluation of significant variables by Plackett-Burman design

Inulinase production regulating significant media components as well as process parameters with respect to their main effects were screened out by Plackett–Burman design. This experimental design identifies the crucial physio-chemical parameters required for elevated inulinase production by investigating n variables in n + 1 experiment (Plackett and Burman, 2018). The levels at which each independent variable was tested is shown in Table 1 and is revealed by equation

$$xi = (Xi - X_0) / \Delta Xi \quad (1)$$

where, xi is the coded value of an independent variable; Xi is the actual value of variable; X₀ is the realvalue of an independent variable at the centre point; Δ Xi is the step change in Xi; i = 1, 2, 3. A total of 11 variables (Inulin, Na₂HPO₄, *Agave sisalana* extract, *Tithonia rotundifolia* Extract, *Cosmos bipinnatus* Extract, NaNO₃, Yeast Extract, K₂HPO₄, MgSO₄, Temperature and pH) were screened in 12 experimental runs

Table 1

Coded and actual levels of variables showing media components used in Plackett-Burman design.

Parameters		Levels of variables			
Variables	Units	Coded Low	Mean	Coded High	
A	Inulin	%	–1 ↔ 1.00	0 ↔ 2.00	+1 ↔ 3.00
B	Na ₂ HPO ₄	%	–1 ↔ 0.25	0 ↔ 0.6250	+1 ↔ 1.00
C	<i>Agave sisalana</i> extract	%	–1 ↔ 4.00	0 ↔ 6.00	+1 ↔ 8.00
D	<i>Tithonia rotundifolia</i> extract	%	–1 ↔ 4.00	0 ↔ 6.00	+1 ↔ 8.00
E	<i>Cosmos bipinnatus</i> extract	%	–1 ↔ 4.00	0 ↔ 6.00	+1 ↔ 8.00
F	NaNO ₃	%	–1 ↔ 1.00	0 ↔ 2.00	+1 ↔ 3.00
G	Yeast Extract	%	–1 ↔ 0.50	0 ↔ 1.00	+1 ↔ 1.50
H	K ₂ HPO ₄	%	–1 ↔ 0.25	0 ↔ 0.6250	+1 ↔ 1.00
J	MgSO ₄	%	–1 ↔ 0.05	0 ↔ 0.100	+1 ↔ 0.15
K	Temperature	OC	–1 ↔ 30.00	0 ↔ 40.00	+1 ↔ 50.00
L	pH	unit	–1 ↔ 6.00	0 ↔ 7.00	+1 ↔ 8.00

Table 2
Plackett-Burman experimental design matrix with experimental values of inulinase production by *Fusarium solani* JALPK.

Run	A %	B %	C %	D %	E %	F %	G %	H %	J %	K OC	L unit	Actual Enzyme activity EU/ml	Predicted Enzyme activity EU/ml
1	1	1	-1	1	1	1	-1	-1	-1	1	-1	1737	1767.13
2	1	1	1	-1	-1	-1	1	-1	1	1	-1	2182.22	2212.35
3	-1	1	1	-1	1	1	1	-1	-1	-1	1	1342.22	1346.3
4	1	-1	1	1	-1	1	1	1	-1	-1	-1	2164.44	2160.37
5	-1	1	1	1	-1	-1	-1	1	-1	1	1	2533.34	2503.21
6	1	-1	-1	-1	1	-1	1	1	-1	1	1	1657.76	1627.63
7	-1	1	-1	1	1	-1	1	1	1	-1	-1	1408.88	1404.81
8	-1	-1	1	-1	1	1	-1	1	1	1	-1	755.55	751.48
9	-1	-1	-1	-1	-1	-1	-1	-1	-1	-1	-1	1053.32	1083.45
10	1	-1	1	1	1	-1	-1	-1	1	-1	1	2044.44	2048.52
11	1	1	-1	-1	-1	1	-1	1	1	-1	1	962.22	932.09
12	-1	-1	-1	1	-1	1	1	-1	1	1	1	917.76	921.84

Code expansion = A:Inulin, B:Na₂HPO₄, C:*Agave sisalana* extract, D:*Tithonia rotundifolia* Extract, E:*Cosmos bipinnatus* Extract, F:NaNO₃, G:Yeast Extract, H:K₂HPO₄, J:MgSO₄, K:Temperature, L:pH.

Table 3
Variables and their levels for the experimental Box-Behnken design (BBD).

Variables	Units	Minimum level	Mean level	Maximum level
A Inulin	%	-1.000 = 1	0 = 2	1.000 = 3
B <i>Agave sisalana</i> extract	%	-1.000 = 4	0 = 6	1.000 = 8
C <i>Tithonia rotundifolia</i> extract	%	-1.000 = 4	0 = 6	1.000 = 8
D NaNO ₃	%	-1.000 = 1	0 = 2	1.000 = 3

Table 4
Box-Behnken design for optimization of parameters acknowledged by the Plackett-Burman design.

Run	A %	B %	C %	D %	Actual enzyme activity EU/ml	Predicted enzyme activity EU/ml
1	1	-1.000	0	0	1739	1650.04
2	0	1	1	0	2662	2684.18
3	1	0	0	-1.000	3203	3251.02
4	-1.000	0	1	0	2149	2327.44
5	0	0	0	0	2656	2421.8
6	0	-1.000	1	0	1415	1449.95
7	0	0	1	-1.000	2716	2538.54
8	1	0	-1.000	0	3167	3086.52
9	1	0	0	1	2537	2605.68
10	0	0	-1.000	-1.000	2601	2568.37
11	1	1	0	0	3132	3129.56
12	-1.000	-1.000	0	0	655.56	512.08
13	-1.000	0	0	-1.000	1763	1742.28
14	0	0	0	0	1975	2421.8
15	0	1	0	-1.000	2383	2437.52
16	0	0	0	0	2304	2421.8
17	0	-1.000	0	1	640	683.44
18	0	0	-1.000	1	1845	1876.54
19	1	0	1	0	2989	3044.18
20	0	0	0	0	2424	2421.8
21	0	1	-1.000	0	2529	2542.02
22	0	-1.000	-1.000	0	800	825.78
23	-1.000	0	0	1	1830	1829.94
24	0	-1.000	0	-1.000	1190	1318.28
25	0	0	0	0	2750	2421.8
26	0	1	0	1	2545	2514.68
27	0	0	1	1	2786	2672.7
28	-1.000	1	0	0	2040	1983.04
29	-1.000	0	-1.000	0	1476	1518.78

A:Inulin, B:*Agave sisalana* extract, C:*Tithonia rotundifolia* extract, D:NaNO₃.

and a smaller, manageable set of factors were obtained by eliminating the insignificant ones. Table 2 represents the experimental matrix design.

2.9. Key ingredient optimization by Box-Behnken methodology

Mathematical correlation between the most significant four variables obtained from Plackett-Burman experiment on inulinase production was developed using methodology (Box and Behnken, 1960). Specified range of four variables used for the optimization was selected as shown in Table 3 along with the Box-Behnken design in the coded and decoded levels of the four variables. The number of experiments (N) required for the development of Box-Behnken design is defined as

$$N = 2k(k - 1) + C0 \tag{2}$$

where k is the number of variables and C0 is the number of central points(Ferreira et al., 2007).The experimental design used for the study is as per Table 4. The experimental plan consisted of 29 runs with five replicates at a central point to fit the second order polynomial model as per eq.

$$Y = \beta_0 + \beta_1 X_1 + \beta_2 X_2 + \beta_3 X_3 + \beta_4 X_4 + \beta_{11} X_1^2 + \beta_{22} X_2^2 + \beta_{33} X_3^2 + \beta_{44} X_4^2 + \beta_{12} X_1 X_2 + \beta_{13} X_1 X_3 + \beta_{14} X_1 X_4 + \beta_{22} X_2 X_3 + \beta_{24} X_2 X_4 + \beta_{34} X_3 X_4 + e \tag{3}$$

where inulinase activity Y is the dependent response variable; inulin (X₁), *Agave sisalana* extract (X₂), *Tithonia rotundifolia* extract (X₃) and NaNO₃ of the medium (X₄) were selected independent variables; β₀ was intercept, β₁, β₂, β₃ and β₄ were linear coefficients, β₁₁, β₂₂, β₃₃ and β₄₄ were squared coefficients, β₁₂, β₁₃, β₁₄, β₂₃, β₂₄ and β₃₄ were interaction coefficients and e was the error of model. Flasks were analyzed for inulinase activity after incubation at 30 °C for 96 h. Control reactors were also carried out to discount if enzyme activity already present prior fermentation. All the experiments were done in duplicate and the average of inulinase production obtained was taken as the response (Y).

2.10. Statistical software used

Design Expert Version 10.0.0 (Stat-Ease Inc., Minneapolis, Minnesota, USA) software was used to statistically analyze the data generating graphs which highlight the roles played by biosynthetic aspects and physical constraints in elevating the final inulinase yield. The optimum values of process parameters were interpreted and curves showing their interactive effect were obtained using the same software.

2.11. Production profile of inulinase

Inulinase activity, protein content (Lowry et al., 1951) and the fructose released (Roe and Papadopoulos, 1954) during bioconversion of *Tithonia rotundifolia* weeds by *Fusarium solani* JALPK was analyzed in

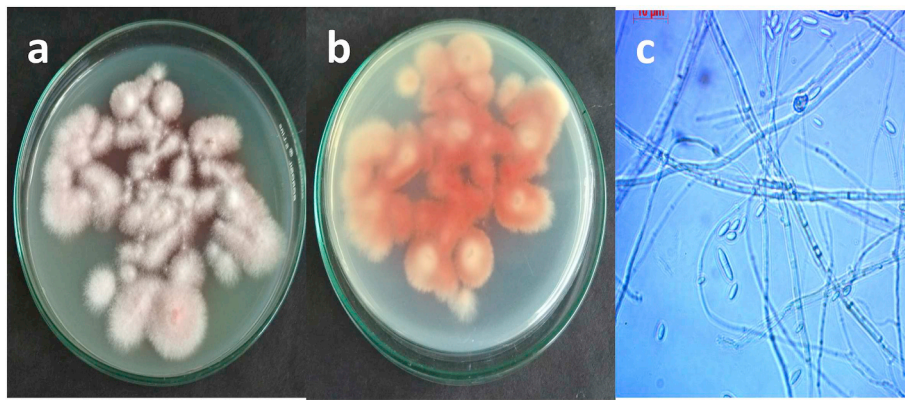


Fig. 1. Morphological characterization of the *Fusarium solani* JALPK grown on PDA medium a. Positive side of the culture plate; b. Reverse side of the culture plate; c. Microphotographs of septate filamentous mycelium with crescent moon shaped spores produced by potent inulinase producing *Fusarium solani* JALPK.

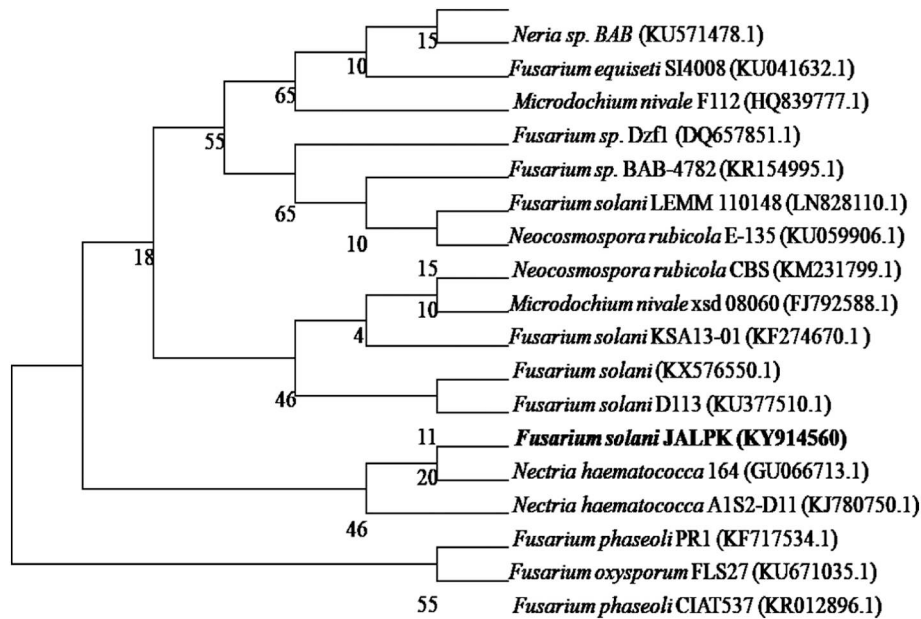


Fig. 2. Phylogenetic tree constructed from 18S rRNA gene sequences of *Fusarium solani* JALPK using the neighbor-joining approach. The bootstrap confidence values corresponding to the scale bar of branch lengths is indicated by the number at all nodes. MEGA 5.1 was employed to conduct phylogenetic analyses.

Table 5
ANOVA results of the Plackett-Burman experimental design to improve fungal inulinase yield.

Analysis of variance table						
Source	Sum of squares	df	Mean square	F-value	p-value	
						Prob > F
Model	3.71E + 06	9	4.13E + 05	148.79	0.0067	Significant
A-Inulin	6.24E + 05	1	6.24E + 05	225.1	0.0044	
B-Na2HPO4	2.06E + 05	1	2.06E + 05	74.31	0.0132	
C-Agave sisalana extract	8.99E + 05	1	8.99E + 05	324.32	0.0031	
D-Tithonia rotundifolia Extract	6.78E + 05	1	6.78E + 05	244.51	0.0041	
E-Cosmos bipinnatus Extract	62,705.79	1	62,705.79	22.61	0.0415	
F-NaNO3	7.50E + 05	1	7.50E + 05	270.58	0.0037	
G-Yeast Extract	28,754.21	1	28,754.21	10.37	0.0844	
J-MgSO4	4.10E + 05	1	4.10E + 05	147.69	0.0067	
K-Temperature	54,420.15	1	54,420.15	19.62	0.0474	
Residual	5546.54	2	2773.27			
Cor Total	3.72E + 06	11				

Table 6
Regression coefficient of Plackett-Burman experimental design.

Std. dev.	52.66	R-squared	0.9985
Mean	1563.26	Adj R-Squared	0.9918
C.V. %	3.37	Pred R-Squared	0.9463
PRESS	2.00E+05	Adeq Precision	36.439
−2 Log likelihood	107.69	BIC	132.54
		AICc	347.69

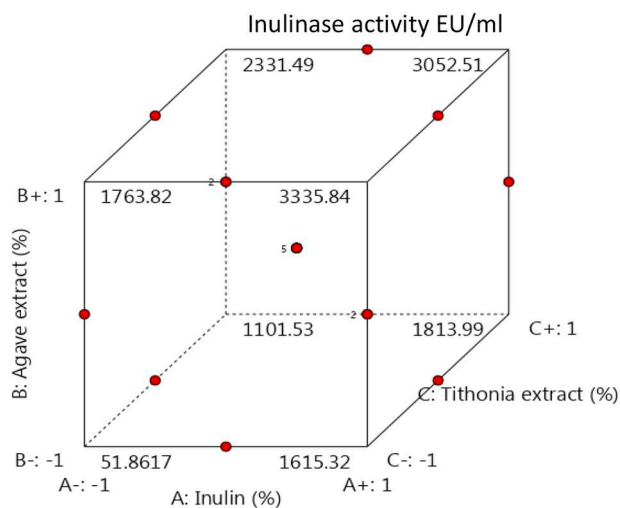


Fig. 3. Cube plot showing the influence of factors relevant to inulinase production.

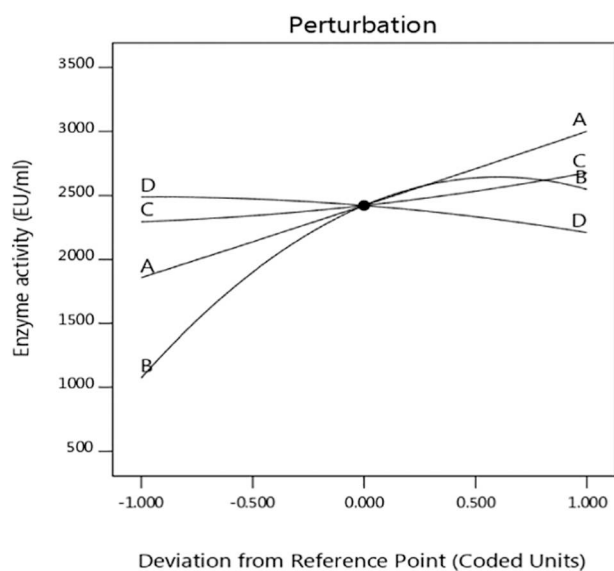


Fig. 4. Perturbation graph implicated in inulinase production.

broth sample harvested at subsequent incubation time of 24 h interval. A graph representing the inulinase production profile at wide range of incubation time was plotted.

2.12. High performance thin layer chromatography

To examine the product of inulin hydrolysis by inulinase HPTLC was carried out using silica gel 60F254 High-performance thin layer chromatography plates (Merck, Germany). Along with the reaction mixture, pure sucrose, fructose and inulin, were used as standards for comparative analysis of the hydrolysate formed by *Fusarium solani* JALPK

after fermentation in both media before optimization and that optimized using response surface methodology. The ascending development solvent used consists of butanol:ethanol:water (50:30:20,v/v). The sugars were visualized by spraying aniline diphenylamine reagent (diphenylamine 1%, aniline 1%, phosphoric acid 10% in 100 mL of acetone) and exposing the plate at 85 °C for about 10 min (Singh et al., 2013).

2.13. Osazone formation test

The formation of distinctive osazones (crystalline derivatives) in the phenyl hydrazine reactions is an important and simplest test for sugar identification. The fermented broth along with the standard fructose was subjected to this test for the qualitative determination of sugar (Hassid and McCreedy, 1942).

2.14. Fourier transform infrared

Fourier transform infrared [FTIR] analysis of standard fructose (Merck) and fermented broth was carried out using a Shimadzu 8400S spectrophotometer, absorption mode between 500 and 4000 cm^{-1} , resolution 4 cm^{-1} , 16 scans. The absorption bands in the mid-infrared region (885 and 1700 cm^{-1}) are characteristic specific functional groups of carbohydrate. A given compound in a mixture can be fingerprinted on the bases of stretching, bending and wagging molecular vibrations of these bands (Kelly and Downey, 2005).

3. Results

3.1. Isolation of the novel inulinolytic fungus

Out of the 15 isolated inulinolytic soil fungi, strain JALPK was found to grow luxuriantly on media containing varying natural inulin rich substrates like *Tithonia rotundifolia*, *Cosmos bipinnatus* and *Agave sisalana* producing relatively high level of inulinase required to degrade these substrates. The inulinase yielding ability of all isolates was checked and the efficient, strain JALPK, was elected to be identified and explored further. When cultivated on PDA the pure culture of strain JALPK produces dry white villi-form filamentous septate mycelium (Fig. 1a). The reverse surface of this culture plate shows development of reddish–pink pigmentation (Fig. 1b). As shown in Fig. 1c, the strain JALPK produced crescent moon shaped spores. Therefore, from this characterization the fungal strain JALPK was identified primarily as *Fusarium* genus.

3.2. Phylogenetic analysis

The nucleotide sequences derived from 18S rRNA were deposited in the GenBank database and accession number KY914560 was assigned to it. Depending on nucleotide homology and comparative investigation of 18S rRNA gene sequence, 98% similarity was displayed by the fungal isolate JALPK with the reference sequence of *Fusarium solani* D113. Hence, the isolate was identified and consequently termed as *Fusarium solani* JALPK. The phylogenetic origin of fungal isolate *Fusarium solani* JALPK is represented in Fig. 2. The values mentioned next to the branches define the percentage of replicate trees in which the allied taxa are clustered together in the bootstrap test (1000). Thus, on the basis of morphological characterization, 18S rRNA gene sequence and phylogenetic analysis, the isolate was confirmed to be *Fusarium solani* JALPK.

3.3. Evaluation of significant variables by Plackett-Burman design

Statistical method for media optimization was performed to boost the inulinase production by *Fusarium solani* JALPK. The responses obtained in terms of inulinase activity, estimated by DNS method are

Table 7
ANOVA results for the model predicted for maximum inulinase synthesis.

Analysis of variance for Response Surface Quadratic model						
Source	Sum of squares	df	Mean square	F-Value	p-Value	
					Prob > F	
Model	1.45E+07	14	1.04E+06	27.36	< 0.0001	Significant
A-Inulin	3.91E+06	1	3.91E+06	103.46	< 0.0001	
B-Agave sisalana extract	6.53E+06	1	6.53E+06	172.58	< 0.0001	
C-Tithonia rotundifolia extract	4.41E+05	1	4.41E+05	11.64	0.0042	
D-NaNO ₃	2.33E+05	1	2.33E+05	6.17	0.0263	
AB	18.32	1	18.32	4.84E-04	0.9828	
AC	1.81E+05	1	1.81E+05	4.79	0.0462	
AD	1.34E+05	1	1.34E+05	3.55	0.0805	
BC	58,081.00	1	58,081.00	1.54	0.2357	
BD	1.27E+05	1	1.27E+05	3.35	0.0886	
CD	1.71E+05	1	1.71E+05	4.51	0.052	
A ²	395.99	1	395.99	0.01	0.92	
B ²	2.42E+06	1	2.42E+06	63.99	< 0.0001	
C ²	27,084.51	1	27,084.51	0.72	0.4117	
D ²	33,983.39	1	33,983.39	0.9	0.3593	
Residual	5.30E+05	14	37,831.97			
Lack of Fit	1.54E+05	10	15,357.08	0.16	0.9907	Not significant
Pure Error	3.76E+05	4	94,019.20			
Cor Total	1.50E+07	28				

Thus confirming that model is significant at the level 96%; CV = 8.97%; Adj- R² = 0. 929; Pred R-Square = 0.90; Adeqprecision = 19.58.

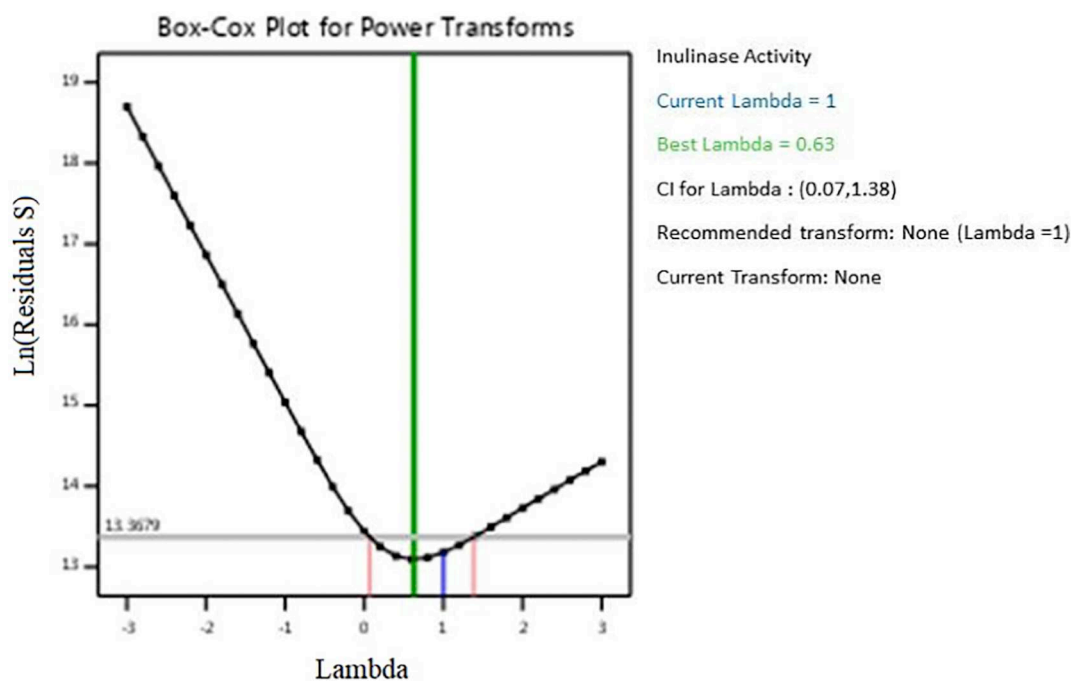


Fig. 5. Box-Cox plot for power transformation in inulinase response.

represented in Table 2. The regression coefficients obtained from ANOVA analysis of 12 Plackett-Burman experiments explains that A, B, C, D, E, F, J, K were significant model terms (Table 5), greatly influencing the inulinase production by *Fusarium solani* JALPK. The Model F-value of 148.79 implies that the model is significant and there is only a 0.67% chance that an F-value this large could occur due to noise. Table 6 shows that the “Pred R-Squared” of 0.9463 was in reasonable agreement with the “Adj R-Squared” of 0.9918; i.e. the difference was < 0.2. “Adeq Precision” measures the signal to noise ratio. A ratio > 4 was desirable. In present study the ratio of 36.439 obtained indicates an adequate signal. Thus confirms, that this model can be used to navigate the design space. Statistical evaluation of experimental data shows that the variables with P value < 0.05 and confidence levels

above 99% were considered to have a significant effect on inulinase production. Therefore, [Inulin (P = 0.0044), Agave sisalana extract (P = 0.0031), Tithonia rotundifolia extract (P = 0.0041) and NaNO₃ (P = 0.0037)] were hence considered as most significant while the remaining components were considered to be insignificant. These most significant 4 variables were selected for further investigation to improve enzyme production by RSM using the Box–Behnken design. It was also assumed that the less significant variables (Na₂HPO₄, Cosmos Extract, Yeast Extract, MgSO₄ and Temperature) in Plackett-Burman design did not require additional optimization treatments. After exclusion of the insignificant model terms the predicted regression equation generated from obtained data is as follows

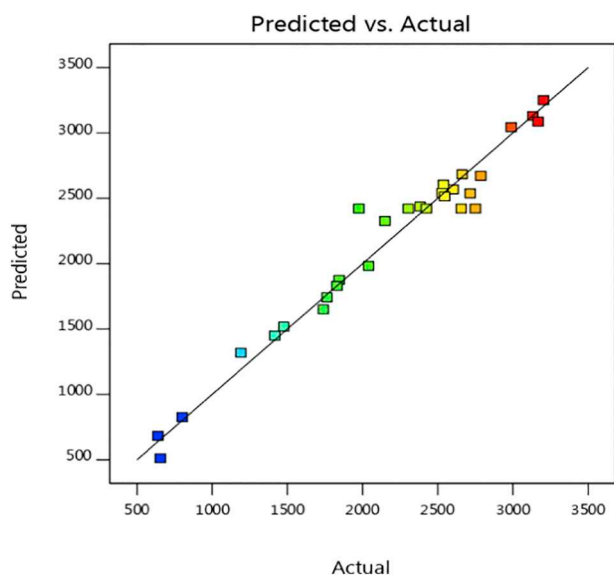


Fig. 6. Parity plot representing the distribution of experimental vs. predicted values of inulinase production.

$$\begin{aligned}
 \text{Enzyme activity} = & +73.43694 + 228.08417 \text{ Inulin} + 349.46889 \text{ Na}_2\text{HPO}_4 \\
 & + 136.88625 \text{ Agave sisalana extract} \\
 & + 118.85708 \text{ Tithonia rotundifolia Extract} \\
 & - 36.14375 \text{ Cosmos extract} - 250.06417 \text{ NaNO}_3 \\
 & + 97.90167 \text{ Yeast Extract} - 3695.01667 \text{ MgSO}_4 \\
 & + 6.73425 \text{ Temperature}
 \end{aligned} \quad (4)$$

3.4. Response surface methodology (RSM)

The adequacy of the model and identification of parameters with statistically significant effects obtained from the Box-Behnken design was conducted by Fisher's test for ANOVA. The maximal inulinase activity at a point (A + B + C) located in the top right is shown in the cube plot (Fig. 3) where 3335.84 EU/mL was the predicted enzyme activity. Perturbation graphs moderates the effect of every factor affecting inulinase biosynthesis by *Fusarium solani* JALPK on a particular point using space design. The response is graphically shown by varying one factor while other factors remain constant (Fig. 4). The levels of inulinase production can be predicted by second-order regression equation represented as follows:

$$\begin{aligned}
 \text{Enzyme activity} = & -7178.51500 + 1538.19667 \text{ Inulin} \\
 & + 2202.23000 \text{ Agave sisalana extract} \\
 & + 88.93667 \text{ Tithonia rotundifolia extract} \\
 & - 636.89000 \text{ NaNO}_3 \\
 & + 1.07000 \text{ Inulin} * \text{ Agave sisalana extract} \\
 & - 106.37500 \text{ Inulin} * \text{ Tithonia rotundifolia extract} \\
 & - 183.25000 \text{ Inulin} * \text{ NaNO}_3 - 30.12500 \\
 & \text{ Agave sisalana extract} * \text{ Tithonia rotundifolia extract} \\
 & + 89.00000 \text{ Agave sisalana extract} * \text{ NaNO}_3 \\
 & + 103.25000 \text{ Tithonia rotundifolia extract} * \text{ NaNO}_3 \\
 & + 7.81333 \text{ Inulin}^2 - 152.73417 \text{ Agave sisalana extract}^2 \\
 & + 16.15458 \text{ Tithonia rotundifolia extract}^2 - 72.38167 \text{ NaNO}_3^2
 \end{aligned} \quad (5)$$

ANOVA (Table 7) for inulinase activity, (Y1) indicated F values of 27.36, which implies the model is significant. There is only a 0.01% chance that an F-value this large could occur due to noise. Model terms are having values of $\text{Prob} > F < 0.05$, which are considered to be significant. The Box-Cox plot of inulinase was 1 as denoted in Fig. 5. A

difference of only 0.37 was observed between the current obtained and best lambda values as shown in the model diagnostic plots. Thus, no power transformation was required for inulinase before formulation of medium through desirability approach. There by, suggesting satisfactory fitness of this model for inulinase response produced by *Fusarium solani* JALPK. Coefficient R (Brkljaca et al., 2014) was determined to check the goodness of fit of the model. An R^2 value of 0.9647 indicated that this model explains 96.47% of data variability in the response Y1. The “Pred R-Squared” of 0.9020 is in reasonable agreement with the “Adj R-Squared” of 0.9295; i.e. the difference is < 0.2 . “Adeq Precision” measures the signal to noise ratio. A ratio > 4 is desirable. In present study the ratio is 19.580 indicating an adequate signal. An agreeable relationship between experimental values and predicted values is signified by the parity plot (Fig. 6). As there is small deviation between the experimental and predicted values, the points have clustered around the diagonal indicating good fit of the model. Thus, ensuring accuracy and applicability of the Box- Behnken design for process optimization of inulinase.

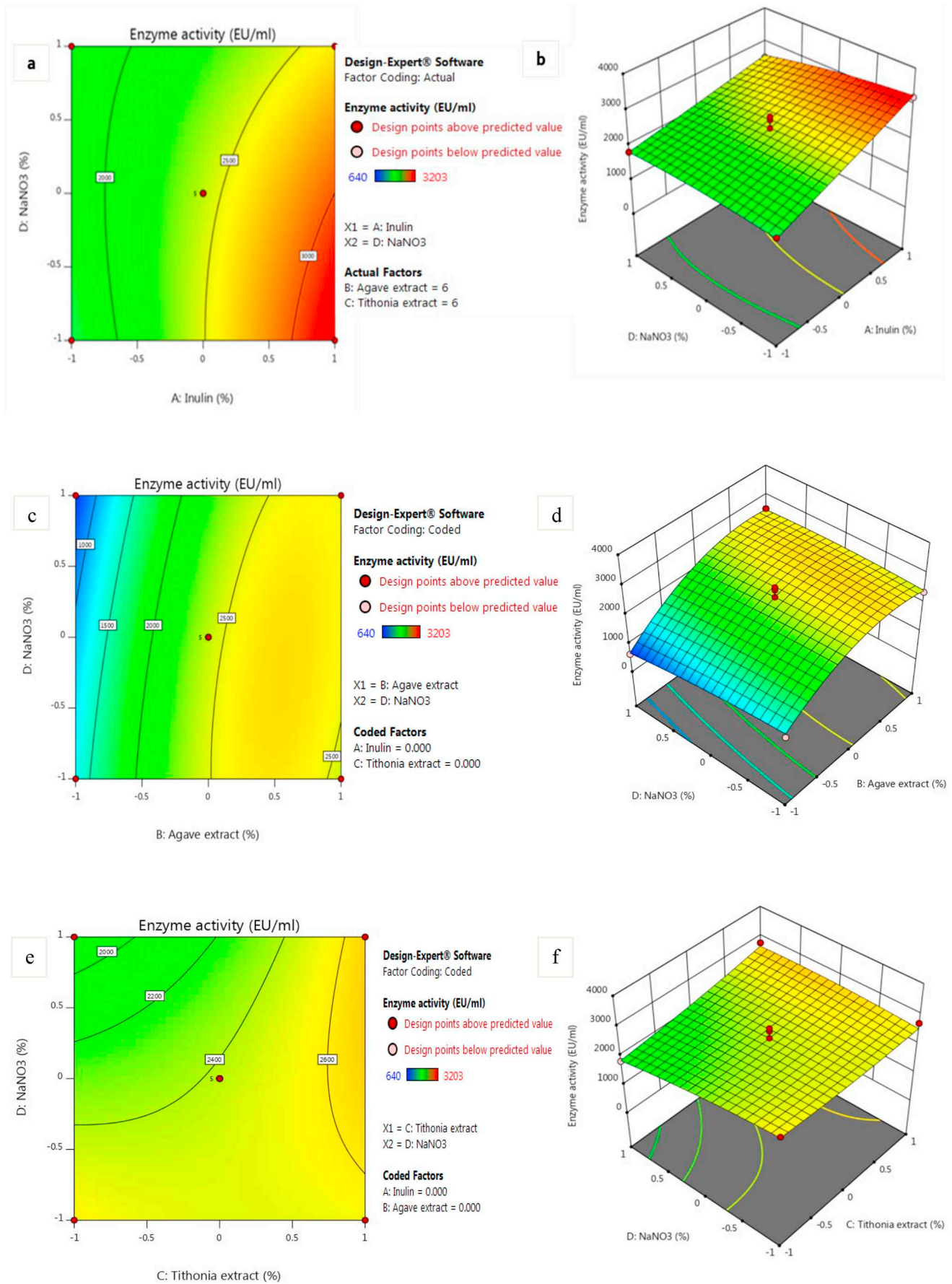
3.5. Interactive effects between significant variables

The interactive effects of variables on inulinase production against any two independent variables, while keeping the other variables at its central (0) level for the inulinase production by *Fusarium solani* JALPK were studied by plotting 3D surface curves of the response (inulinase production). Contour plots from the interactions between the variables were also presented. Fig. 7a and b shows that NaNO_3 and synthetic inulin within the range tested improves inulinase production. Maximum inulinase yield was achieved as inulin % increased up to 3%. Change in $\text{NaNO}_3\%$ did not alter the enzyme synthesis thus restricting the addition of this component in the media to lower limits. The effect due to variation in the concentration of NaNO_3 and *Agave sisalana* extract on inulinase production is shown in Fig. 7c and d. A steep reduction in inulinase production was recorded as we moved down from 8 to 4% of *Agave sisalana* extract and no effect of varying NaNO_3 concentration was observed on the enzyme synthesis. Thus, it can be concluded that the enzyme production is stimulated at relatively low nitrogen concentration and remained unaffected even if the % exceed up to 3% and increasing *Agave sisalana* extract level enhances the enzyme production. Fig. 7e and f shows the interactions with *Tithonia rotundifolia* extract as carbon source and NaNO_3 as nitrogen source. Elevation in inulinase production was observed with increasing *Tithonia rotundifolia* extract concentration (4% to 8%) but the enzyme activity remained steady at various NaNO_3 concentrations (1% to 3%). This explains that there is no need of supplementing high concentration of nitrogen source in the media in presence of *Tithonia rotundifolia* extract.

Fig. 7g and h, show the response surface plots as functions of *Agave sisalana* extract versus inulin, for inulinase production. Inulinase was largely synthesized at 6–7% of *Agave sisalana* extract while there was observed increase in the production as the inulin % increased from 1 to 3%. The effects on inulinase production due to change in the concentration of *Tithonia rotundifolia* extract and inulin are visualized in Fig. 7i and j. Maximum enzyme was produced by utilizing *Tithonia rotundifolia* extract readily as substrate even in the presence of synthetic inulin in media. Inulinase production increases with simultaneous increase in the concentrations of *Tithonia rotundifolia* extract and inulin from 4% to 8% and 1% to 3%, respectively. Fig. 7k and l reveals that the enzyme activity was enhanced greatly due to rapid utilization of *Tithonia rotundifolia* extract by *Fusarium solani* JALPK than that of the *Agave sisalana* extract.

3.6. Production profile of inulinase

The production of extracellular inulinase after inoculation of *Fusarium solani* JALPK was monitored in both statistically optimized and non-optimized fermented broth (Fig. 8). The products formed in the



(caption on next page)

Fig. 7. Contour plots and Response surface 3 D graphs of inulinase production from *Fusarium solani* JALPK showing interactive effects of NaNO₃ and inulin (a & b): NaNO₃ and *Agave sisalana* extract (c & d): NaNO₃ and *Tithonia rotundifolia* extract (e & f): *Agave sisalana* extract and inulin (g & h): *Tithonia rotundifolia* extract and inulin (i & j): *Tithonia rotundifolia* extract and *Agave sisalana* extract (k & l) respectively.

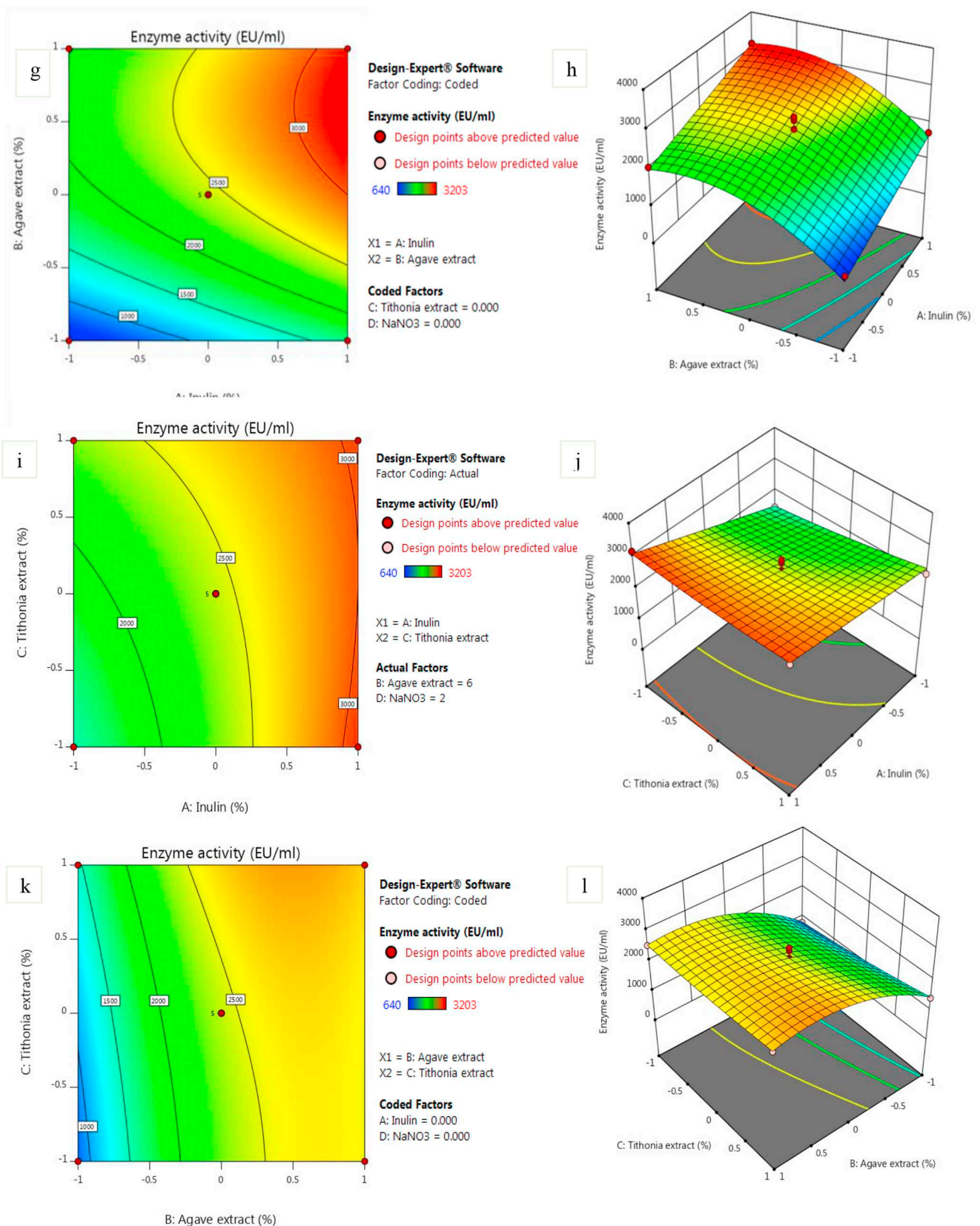


Fig. 7. (continued)

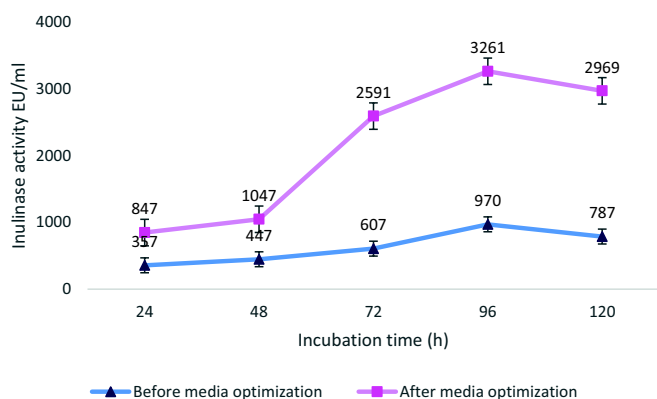


Fig. 8. Time course outline of inulinase from *Fusarium solani* JALPK by submerged fermentation (SmF) in optimized and non-optimized fermented broth.

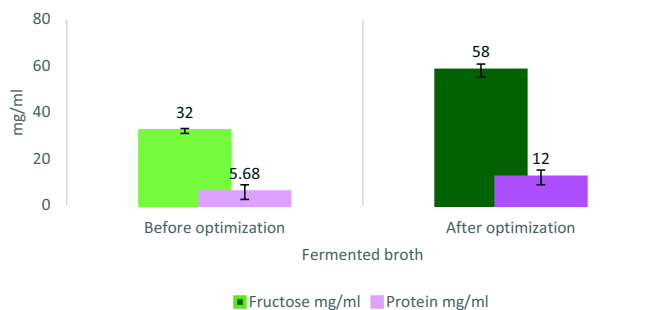


Fig. 9. Comparative study of product released by *Fusarium solani* JALPK in fermented broth before and after statistical optimization.

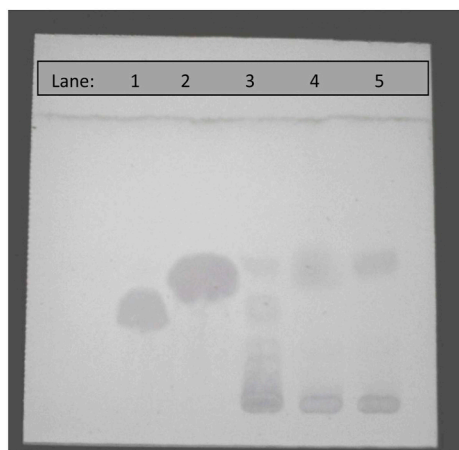


Fig. 10. End product analysis after action of *Fusarium solani* JALPK synthesized inulinases using HPTLC. Lane (1) Standard sucrose, (2) Standard fructose, (3) Standard inulin, (4) Fermented broth before media optimization and (5) Fermented broth after media optimization using RSM.

broth (proteins and fructose specifically) during the breakdown process of inulin rich weeds were also estimated by withdrawing the samples at after every 12 h interval (Fig. 9).

3.7. High performance thin layer chromatography

The qualitative examination of hydrolyzed products formed after inulin hydrolysis by inulinase from *Fusarium solani* JALPK was done by HPTLC. The developed HPTLC plate (Fig. 10) loaded with hydrolyzed mixture showed only one spot corresponding to the level up to that obtained for standard fructose.

3.8. Osazone formation test

Characteristic needle shaped crystals resulting from the reaction of sugars having free carbonyl group with phenyl hydrazine formed in fermented broth was same as that formed in standard fructose solution. Fig. 11 represents the Osasones.

3.9. Fourier transform infrared

The observed absorption bands in standard fructose (Fig. 12) after Fourier Transform infrared analysis were 610, 689, ($\text{C}=\text{C}-\text{H}$, $\text{C}-\text{H}$ bend) 772, 1219, 1293, 1381, ($\text{C}-\text{O}$ stretch) 1442, ($\text{C}-\text{H}$ bend) 1457, 1502, $\text{C}-\text{C}$ stretch 1548, 1641, 1658, $\text{C}=\text{C}$ stretch 1725, $\text{C}=\text{O}$ stretch 1765, 1853, 3345 cm^{-1} ($\text{O}-\text{H}$ stretch $\text{C}-\text{H}$ stretch).

4. Discussion

Amongst the 15 isolates obtained from rhizospheric soil of various weeds, the most efficient isolate secreting maximum amount of inulinase after hydrolyzing inulin rich weed was identified to be *Fusarium solani* JALPK. Response Surface Methodology for media optimization was performed to boost the inulinase production by *Fusarium solani* JALPK. The experimental data evaluates that the model and the design implemented suits well and helps in inducing the process optimization of inulinase. The 3D contour plots obtained show the interactions between the significant factors. Low inulinase productivity was recorded at the extreme levels of *Agave sisalana* extract (i.e. 3% and 8%) but at *Agave sisalana* extract concentration of about 6–7% there was increase in the response. The lower substrate concentration may not be satisfying the organisms need and the higher concentration may be imparting a repressive catabolic action on inulinase production. Whereas a consistent boosting of inulinase synthesis was observed in the media containing up to 8% *Tithonia rotundifolia* extract. Thus *Tithonia rotundifolia* was attacked by *Fusarium solani* JALPK first and to the highest extend than other inulin rich substrates. As reported earlier (Kamble et al., 2018), *Tithonia rotundifolia* extract effectively induces privileged inulinase production by *Arthrobacter mysorens* strain no.1 within 48 h under SmF at 30 °C. But there is no scientific reference available regarding utilization of *Tithonia rotundifolia* weed by *Fusarium* spp. Hence it is difficult to compare the present results with any other published data. Table 8 highlights on the inulinase activity by various fungal strains when cultivated on different inulin rich substrates. This is the first report emphasizing on the inulinolytic hydrolysis of *Tithonia rotundifolia* using *Fusarium solani* JALPK yielding fructose.

The validation for inulinase production was made using this statistically predicted medium. Therefore, *Fusarium solani* JALPK was inoculated in this medium and inulinase production was estimated after every regular incubation interval. The profitably validation was achieved as the predicted values by the model were in good conformity with the obtained response. The model predicted a maximum inulinase production of 3261.011 EU/mL in a medium containing Inulin 2.846, *Agave sisalana* extract 5.819, *Tithonia rotundifolia* extract 4.185 and NaNO_3 1.099%. Thus, after RSM obtained model validation, an overall 3.36 fold increase in inulinase production was predicted signifying an easy scale-up of inulinase production by optimized conditions. HPTLC results indicate the exoinulinolytic nature of inulinase synthesized by *Fusarium solani* JALPK that completely hydrolyses inulin from media into fructose. Such pattern of fungal exoinulinase activity was also discussed in previous report (Kamble et al., 2017). Literature emphasizing on the exoinulinolytic nature of several fungal species like *Penicillium subrubescens* (Mansouri et al., 2013) *Chrysosporium pannorum* (Xiao et al., 1989) *Aspergillus tritici* BGPUP6 (Singh et al., 2016) using raw *Asparagus* inulin (Sarup et al., 2016) and *A. tubingenensis* (Trivedi et al., 2012) are also accessible. The inulinase from *Fusarium solani* JALPK hydrolyzed the *Tithonia* weed by releasing fructose in the fermented broth which was validated by performing HPTLC. This confirms

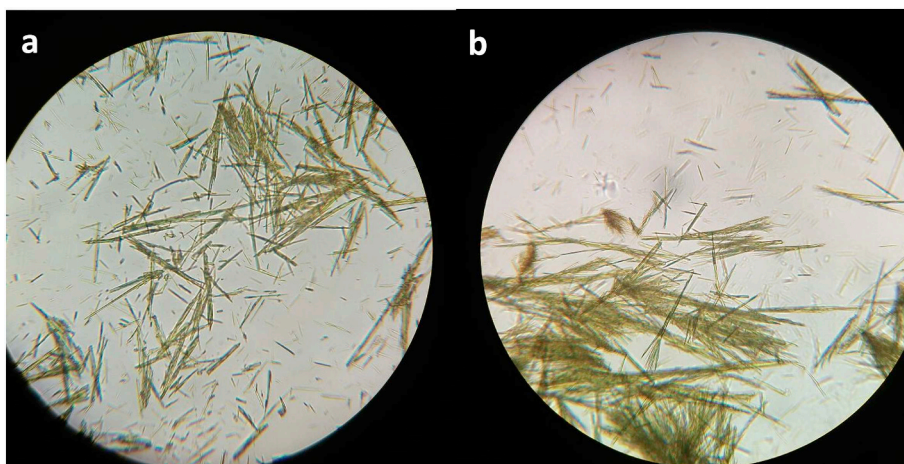


Fig. 11. Microscopic Appearance of Crystalline Osazones observed in.
 a) standard Fructose solution.
 b) Statistically optimized broth fermented by *Fusarium solani* JALPK.

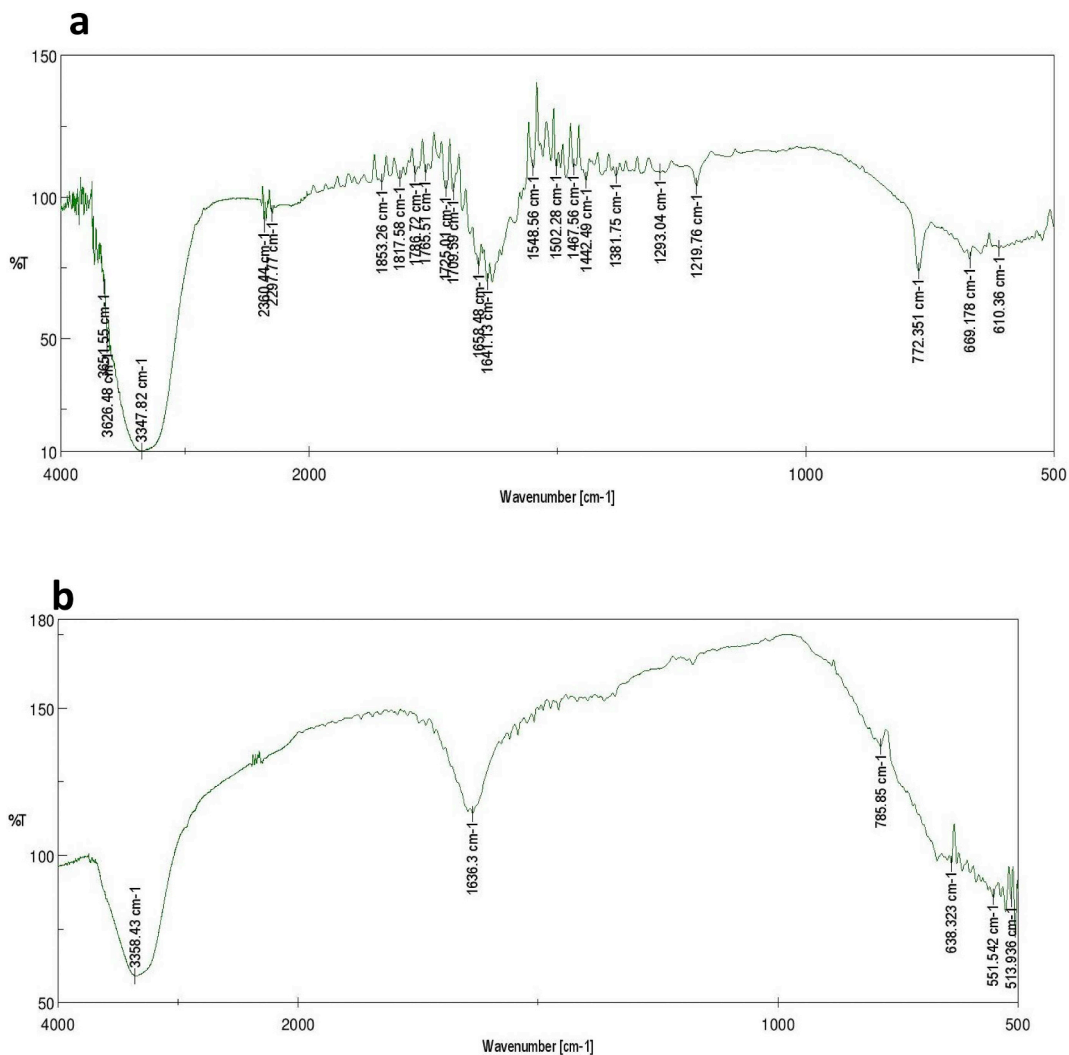


Fig.12. a. FT-IR spectra image of standard fructose. b. FT-IR spectra image of resulting product after fermentation in statistically optimized fermented broth.

Table 8
Comparison of inulinase activity by various fungal strains when cultivated on different substrates.

Sr No.	Fungus	Inulinase activity	Substrate used	Reference
1	<i>Aspergillus fumigatus</i>	3.72 U/ml	Wheat bran	(Gouda, 2002)
2	<i>Aspergillus niger</i> NK-126	52.3 IU/ml	Tap roots of Dandelion (<i>Taraxacum officinale</i>)	(Kango, 2008)
3	<i>Thielaviasterstris</i> NRRL 8126 and <i>Aspergillus foetidus</i> NRRL 337	8.42 U/ml 8.36 U/ml	<i>Cichoriumintybus</i> L. root extract	(Fawzi, 2011)
4	<i>Aspergillus wentii</i>	1.340 U/ml	<i>Jerusalem artichoke</i>	(Karatop and Sanal, 2013)
5	<i>Aspergillus niger</i> 245	2.92 IU/ml	<i>Dahlia</i> extract and pure inulin	(Skowronek and Fiedurek, 2004)
6	<i>Penicillium oxalicum</i> BGPUP-4	322.10 IU per g of dry substrate	Carrot pomace	(Singh et al., 2018)
7	<i>Aspergillus niger</i>	(61 U/ml)	Banana peel	(Kalra and Kumari, 2017)
8	<i>Aspergillus kawachii</i> IFO 4308	35 mU/ml	Yacon (<i>Smallanthus sonchifolius</i>)	(Chesini et al., 2013)
9	<i>Aspergillus niveus</i> Blochwitz 4128 URM	56 U/ml	Synthetic inulin	(Souza-motta et al., 2005)
10	<i>Aspergillus niger</i> van Teighem UV11	290 U/ml	Kuth (<i>Saussurealappa</i>) Defatted groundnut meal, defatted soyabean meal	(Viswanathan and Kulkarni, 1995)
11	<i>Geotrichum candidum</i>	45.62 U/ml	<i>Jerusalem artichoke</i> (JA) (<i>Helianthus tuberosus</i> L.)	(Erdal et al., 2011)
12	<i>Fusarium solani</i> JALPK	3261.011 EU/ml	<i>Tithonia rotundifolia</i> extract	Present study

the exoinulinase nature of this fungal hydrolytic enzyme. These typical osazones formed were also used to correlate with their associated disorders. Like fructose in people on high fruit diet, in patients with hereditary fructose intolerance and essential fructosuria and may other carbohydrate related disorders (Steinmann et al., 2015). FTIR spectra denotes that at 1635 cm⁻¹ a key peak corresponding to C=O stretching and –C=C– stretching was detected in the fermented broth which represents the presence of alkenes, carboxylic and ketose functional group (Kacurakova and Mathlouthi, 1996). Thus, confirming the hydrolysis of inulin rich weeds into fructose by exoinulinase released by *Fusarium solani* JALPK. Therefore, it can be exploited commercially to produce inulinase from *Tithonia* weed.

5. Conclusions

In this experiment maximal activity was obtained with medium concentrations of Inulin 2.846, *Agave sisalana* extract 5.819, *Tithonia rotundifolia* extract 4.185 and NaNO₃ 1.09%. Under this optimal condition, the inulinase activity (3261.011 U/mL) obtained predicted by the model agreed very well with experimental data, confirming its validity, with a 3.36 fold increase in inulinase activity achieved by optimization of the culture medium composition. This statistical approach has established a major contribution in inulinase production by optimizing independent factors. It is a first reference on the enhanced production of inulinase by *Fusarium solani* JALPK using *Tithonia rotundifolia* weed as a cost-effective substrate for fructose formation.

Conflict of interest

The authors declare that they have no conflicts of interest.

Acknowledgments

Authors are thankful to Shivaji University, Kolhapur, for granting Golden Jubilee Research Fellowship as a financial support to execute the present work.

References

- Box, G.E.P., Behnken, D., 1960. Some new three level designs for the study of quantitative variables Society for Quality. *Technometrics* 2, 455–475. <http://www.jstor.org/stable/1266454>.
- Brkljaca, J., Bodroza-Solarov, M., Krulj, J., Terzic, S., Mikic, A., Marjanovic Jeromela, A., 2014. Quantification of inulin content in selected accessions of *Jerusalem Artichoke* (*Helianthus tuberosus* L.). *HELIA* 37 (60), 105–112.
- Chesini, M., Paola, L., Dante, N., 2013. *Aspergillus kawachii* produces an inulinase in cultures with yacon (*Smallanthus sonchifolius*) as substrate. *Electron. J. Biotechnol.* 16, 1–13. <https://doi.org/10.2225/vol16-issue3-fulltext-13>.
- Erdal, S., Canli, O., Algur, O.F., 2011. Inulinase production by *Geotrichum candidum*

- using Jerusalem artichoke as sole carbon source. *Rom. Biotechnol. Lett.* 16, 6378–6383.
- Fawzi, E.M., 2011. Comparative study of two purified inulinases from thermophile *Thielaviasterstris* NRRL 8126 and mesophile *Aspergillus foetidus* NRRL 337 grown on *Cichoriumintybus* L. *Braz. J. Microbiol.* 42 (2), 633–634. <https://doi.org/10.1590/S1517-838220110002000028>.
- Ferreira, S., Bruns, R., Ferreira, H., 2007. Box-Behnken design: an alternative for the optimization of analytical methods. *Anal. Chim. Acta* 597, 179–186. <https://doi.org/10.1016/j.aca.2007.07.011>.
- Gouda, M., 2002. Some properties of Inulinase from *Aspergillus fumigatus*. *Pak. J. Biol. Sci.* 5 (5), 589–593. <https://doi.org/10.3923/pjbs.2002.589.593>.
- Hafizi, R., Salleh, B., Latifah, Z., 2013. Morphological and molecular characterization of *Fusarium solani* and *F. oxysporum* associated with crown disease of oil palm. *Braz. J. Microbiol.* 44 (3), 959–968. <https://doi.org/10.1590/S1517-83822013000300047>.
- Hanover, L., White, J., 1993. Manufacturing, composition and applications of fructose. *Am. J. Clin. Nutr.* 58 (5), 724S–732S. <https://doi.org/10.1093/ajcn/58.5.724S>.
- Hassid, W.Z., McCreedy, R.M., 1942. Identification of sugars by microscopic appearance of crystalline Osazones. *Ind. Eng. Chem. Anal. Ed.* 14, 683–686. <https://doi.org/10.1021/i560108a025>.
- Howlett, B.J., Knox, R.B., Heslop-Harrison, J., 1973. Pollen-wall proteins: release of the allergen antigen E from intine and exine sites in pollen grains of ragweed and *Cosmos*. *J. Cell Sci.* 13, 603–619.
- Kacurakova, M., Mathlouthi, M., 1996. FTIR and laser-Raman spectra of oligosaccharides in water: characterization of the glycosidic bond. *Carbohydr. Res.* 284, 145–157. [https://doi.org/10.1016/0008-6215\(95\)00412-2](https://doi.org/10.1016/0008-6215(95)00412-2).
- Kalra, K., Kumari, R., 2017. Isolation and production of inulinase from banana peel by using *Aspergillus niger* under submerged. *Int. J. Sci. Res. Publ.* 7, 446–454. <https://doi.org/10.293220>.
- Kamble, P., Jadhav, J., Attar, Y., 2017. Comparison of optimization conditions for elevated bacterial and fungal inulinase. *Int. J. Res. Biosci.* 5, 225–228 *Agriculture and Technology*.
- Kamble, P.P., Kore, M.V., Patil, S.a., Jadhav, J.P., Attar, Y.C., 2018. Statistical optimization of process parameters for inulinase production from *Tithonia* weed by *Arthrobacter mysorens* strain no.1. *J. Microbiol. Methods* 149, 55–66. <https://doi.org/10.1016/j.jmimet.2018.04.019>.
- Kango, N., 2008. Production of inulinase using tap roots of dandelion (*Taraxacum officinale*) by *Aspergillus niger*. *J. Food Eng.* 85, 473–478. <https://doi.org/10.1016/j.jfoodeng.2007.08.006>.
- Karatop, R., Sanal, F., 2013. A potential resource in fructose production from inulin: *Aspergillus wentii* inulinase. *J. Cell. Biol. Mol.* 11, 21–28. <http://jcm.b.halic.edu.tr>.
- Kelly, J.F.D., Downey, G., 2005. Detection of sugar adulterants in apple juice using fourier transform infrared spectroscopy and chemometrics. *J. Agric. Food Chem.* 53, 3281–3286. <https://doi.org/10.1021/jf048000w>.
- Kovaleva, T.A., Holyavka, M.G., Bogdanova, S.S., 2009. Inulinase immobilization on macroporous anion-exchange resins by different methods. *Bull. Exp. Biol. Med.* 148, 39–41. <https://doi.org/10.1007/s10517-009-0623-y>.
- Lingyun, W., Jianhua, W., Xiaodong, Z., Da, T., Yalin, Y., Chenggang, C., Tianhua, F., Fan, Z., 2007. Studies on the extracting technical conditions of inulin from *Jerusalem artichoke* tubers. *J. Food Eng.* 79, 1087–1093. <https://doi.org/10.1016/j.jfoodeng.2006.03.028>.
- Lowry, O.H., Rosebrough, N., Farr, A., Randall, R., 1951. Protein measurement with the Folin phenol reagent. *J. Biol. Chem.* 193, 265–275. <http://www.jbc.org/content/193/1/265.citation>.
- Madden, T., 2013. The BLAST sequence analysis tool. In: *The NCBI Handbook*. Bethesda (MD): National Center for Biotechnology Information (US). vol. 2. pp. 1–12. <http://www.ncbi.nlm.nih.gov/80/BLAST>.
- Mansouri, S., Houbaken, J., Samson, R.A., Frisvad, J.C., Christensen, M., Tuthill, D.E., Koutaniemi, S., Hatakka, A., Lankinen, P., 2013. *Penicillium subrubescens*, a new species efficiently producing inulinase. *Antonie van Leeuwenhoek. Int. J. G. Mol. Microbiol.* 103, 1343–1357. <https://doi.org/10.1007/s10482-013-9915-3>.
- Miller, G.L., 1959. Use of Dinitrosalicylic acid reagent for determination of reducing sugar. *Anal. Chem.* 31, 426–428. <https://doi.org/10.1021/ac60147a030>.

- Muoghalu, J.I., Chuba, D., 2005. Seed germination and reproductive strategies of *Tithonia diversifolia* (Hemsl.) Gray and *Tithonia rotundifolia* (P.M) Blake. Appl. Ecol. Environ. Res. 3, 39–46. <https://doi.org/10.15666/aer/0301>.
- Plackett, R.L., Burman, J., 2018. The Design of Optimum Multifactorial Experiments. Biometrika 33, 305–325. <http://www.jstor.org/stable/2332195>.
- Roe, J.H., Papadopoulos, N., 1954. The determination of fructose 6-phosphate and fructose 1,6-diphosphate. J. Biol. Chem. 210, 703–710. <http://www.jbc.org/content/210/2/703>.
- Saitou, N., Nei, M., 1987. The neighbor-joining method: a new method for reconstructing phylogenetic trees. Mol. Biol. Evol. 4, 406–425.
- Sarup, R., Pal, R., Kennedy, J.F., 2016. International journal of biological macromolecules Endoinulinase production by a new endoinulinase producer *Aspergillus tritici* BGPUP6 using a low cost substrate. Int. J. Biol. Macromol. 92, 1113–1122. <https://doi.org/10.1016/j.ijbiomac.2016.08.026>.
- Seiler, G.J., 2007. The potential of wild sunflower species for industrial uses. Helia 30, 175–198. <https://doi.org/10.2298/HEL0746175S>.
- Selvakumar, P., Pandey, A., 1999. Solid state fermentation for the synthesis of inulinase from *Staphylococcus* sp. and *Kluyveromyces marxianus*. Process Biochem. 34, 851–855. [https://doi.org/10.1016/S0032-9592\(99\)00008-4](https://doi.org/10.1016/S0032-9592(99)00008-4).
- Singh, A., Manju Yadav, A., Bishnoi, N.R., 2013. Statistical screening and optimization of process variables for xylanase production utilizing alkali-pretreated rice husk. Ann. Microbiol. 63, 353–361. <https://doi.org/10.1007/s13213-012-0482-z>.
- Singh, R., Singh, R., Kennedy, J., 2016. Endoinulinase production by a new endoinulinase producer *Aspergillus tritici* BGPUP6 using a low cost substrate. Int. J. Biol. Macromol. 92, 1113–1122. <https://doi.org/10.1016/j.ijbiomac.2016.08.026>.
- Singh, R., Chauhan, K., Singh, J., Pandey, A., Larroch, C., 2018. Solid-state fermentation of *Carrot Pomace* for the production of Inulinase by *Penicilliumoxalicum*BGPUP-4. Food Technol. Biotechnol. 56, 31–39. <https://doi.org/10.1713/ftb.56.01.18.5411>.
- Skowronek, M., Fiedurek, J., 2004. Optimisation of inulinase production by *Aspergillus niger* using simplex and classical method. Food Technol. Biotechnol. 42, 141–146.
- Souza-motta, C.M., Auxiliadora, M., Cavalcanti, Q., 2005. *Aspergillus niveus* Blochwitz 4128URM: new source for inulinase production. Braz. Arch. Biol. Technol. 48, 343–350. <https://doi.org/10.1590/S1516-89132005000300003>.
- Steinmann, B., Gitzelmann, R., Van, den., Berghe, G., 2015. Essential fructosuria, hereditary fructose intolerance, and fructose – 1, 6- diphosphatase deficiency. Metab. Mol. Bases Inherit. Dis. 1–73.
- Tamura, K., Nei, M., Kumar, S., 2004. Prospects for inferring very large phylogenies by using the neighbor-joining method. Proc. Natl. Acad. Sci. 101, 11030–11035. <https://doi.org/10.1073/pnas.0404206101>.
- Tamura, K., Stecher, G., Peterson, D., Filipski, A., Kumar, S., 2013. MEGA6: molecular evolutionary genetics analysis version 6.0. Mol. Biol. Evol. 30, 2725–2729. <https://doi.org/10.1093/molbev/mst197>.
- Thompson, J.D., Higgins, D., Gibson, T., 1994. Clustal-W-improving the sensitivity of progressive multiple sequence alignment through sequence weighting, position-specific gap penalties and weight matrix choice. Nucleic Acids Res. 22, 4673–4680.
- Trivedi, S., Divecha, J., Shah, A., 2012. Optimization of inulinase production by a newly isolated *Aspergillus tubingensis* CR16 using low cost substrates. Carbohydr. Polym. 90, 483–490. <https://doi.org/10.1016/j.carbpol.2012.05.068>.
- Viswanathan, P., Kulkarni, P.R., 1995. Full factorial design to study fermentative production of inulinase using inulin from kuth (*Saussurea lappa*) root powder by *Aspergillus niger* van Teighem UV11 mutant. Bioresour. Technol. 54, 117–121. [https://doi.org/10.1016/0960-8524\(95\)00107-7](https://doi.org/10.1016/0960-8524(95)00107-7).
- Xiao, R., Tanida, M., Takao, S., 1989. Purification and characteristics of two exoinulinases from *Chrysosporium pannorum*. J. Ferment. Bioeng. 67, 331–334. [https://doi.org/10.1016/0922-338X\(89\)90250-X](https://doi.org/10.1016/0922-338X(89)90250-X).